Accepted Manuscript

Title: Bioelectrical impedimetric sensor for single cell analysis based on nanoroughened quartz substrate; suitable for cancer therapeutic purposes

Authors: Milad Gharooni, Mohammad Abdolahad

PII: S0731-7085(17)30827-0
DOI: http://dx.doi.org/doi:10.1016/j.jpba.2017.05.024
Reference: PBA 11278

To appear in: *Journal of Pharmaceutical and Biomedical Analysis*

Received date: 3-4-2017
Revised date: 10-5-2017
Accepted date: 12-5-2017

Please cite this article as: Milad Gharooni, Mohammad Abdolahad, Bioelectrical impedimetric sensor for single cell analysis based on nanoroughened quartz substrate; suitable for cancer therapeutic purposes, Journal of Pharmaceutical and Biomedical Analysishttp://dx.doi.org/10.1016/j.jpba.2017.05.024

Bioelectrical impedimetric sensor for single cell analysis based on nanoroughened quartz substrate; suitable for cancer therapeutic purposes

Milad Gharooni[a,b,#], Mohammad Abdolahad[a,b,*,#]

[a]Nano Electronic Center of Excellence, Nano Bio Electronic Devices Lab, School of Electrical and Computer Eng, University of Tehran, P.O. Box 14395/515,Tehran, Iran

[b]Nano Electronic Center of Excellence, Thin Film and Nanoelectronic Lab, School of Electrical and Computer Eng, University of Tehran, P.O. Box 14395/515,Tehran, Iran

[*]Corresponding Author: M. Abdolahad (m.abdolahad@ut.ac.ir)

[#] Authors with same contribution

Highlights:

- Bioelectrical impedimetric sensor has been fabricated for single cell analysis.
- Single cells applied direct contact by nanoroughened electrodes.
- Effect of anticancer drugs were evaluated on single breast cancer cell by electrical signals.
- Some correlations between electrical responses and cell mitotic activities were achieved.

Abstract

Single cells analysis has been interested in recent decade. Apart from scientific benefits to achieve new biological phenomena in cell study, many diagnostic and therapeutic protocols in non-communicable diseases were introduced by single cell analysis. Moreover, non-invasive methods to maintain the investigated cell for time dependent monitoring has been widely studied because of its importance in some crucial cases such as drug resistance in cancer. Bioelectrical monitoring is one of such methods. Although the procedures reported based on electrical probing might not induce cell disruption, indirect connection between recording electrodes and cell membrane

(mostly in microfluidic approaches) reduced the quality of response and limited the precision of the results. Here, a bioelectronic sensor for monitoring the effect of anticancer drugs on single breast cancer cells was fabricated based on nano-roughened gold electrodes on a quartz substrate applied direct contacts to cell membrane. Whole of the surface except a microcircle surrounded the sensing region was passivated by overbaked photoresist layer. Cells were dropped on the sensor without the assistance of any micropipette or microfluidic systems and just individual regions for attachment of one cell has been opened on the sensing region arrays. MCF-7 cancer cells were time tracked under the effect of Paclitaxel and Mebendazole anti-tubulin drugs in low and high doses. Inducing non regulated depolymerization and polymerization in tubulin structures of the single cancer cells were monitored by the electrical signals recorded before and after drug treatment. Electrical responses of single cells to their incubation with drugs completely reflected their vitality and biological states which were confirmed by confocal imaging. This is one of the first investigation on bioelectrical monitoring of single cell's resistance to anticancer drugs.

Keyword: single cell; biosensor; cancer; extreme drug resistance; impedance; nano roughened surface.

1. Introduction

Heterogeneity of cellular metabolism during disease transformation or therapeutic treatments resulted in increased appreciation on understanding physiological functions of single cells. Decision-making by tracing pathological evidences through a single cell have been made in various diagnostic and therapeutic procedures [1,2]. However, an outstanding challenge for many modern single-cell assays is damaging the cells during the analysis and limitation in time dependent monitoring of a treated cell [3]. The nature of biochemical analysis causes cellular

damaging and lysis [2,3]. Some other non-invasive procedures such as Raman spectroscopy [4] or optical bio sensing [5] involve complicated operating procedures. Also they present insufficient data on biological state of the cell. As being an active and complex electronic system, cells exhibited distinguished electrical behavior during various physiological and pathological states [6]. Moreover, many crucial changes in cell metabolism are highly correlated with electrochemical exchanges between cell's inner and outer parts or bioelectrical changes in cytoskeleton, cytoplasm, nucleus and membrane [7]. The ability to translating cell's physiological or pathological states to electrical patterns would be highly interested for live analysis of single cell. Many modern devices and methods have been introduced for electrical measurement of single cells [8]. A limitation associated with some of these biosensors was the fact that they were based on microfluidic approach in which the cell was held in a solution micro cavity without direct access of the electrodes to its membrane. Locating the cells in desired place between electrodes by micropipette [9] or voltage phase controlled method [10] are some experimentally complicated alternative procedures which reduced the applications of such devices. Also, precise location of the cell between the recording electrodes are crucial to suppress electrical noises in the response of such devices [11]. In this regard, therapeutic treatments (like drug incubation or ray therapy which would biologically induce one of the cell's sub-organelles, might also affect bioelectrical response of exposed cell [12]. Anti-tubulin drugs are considered to be one of the most important groups of anti-cancer drugs. They can cause the obstruction of MTs polymerization (lengthening) or depolymerization (shortening), which highly affects the dynamics of the spindles and results in the mitotic arrest and cell death. Microtubules are involved in a diverse range of cellular functions including mitosis and meiosis, motility, maintenance of cell shape and intracellular trafficking of macromolecules and organelles [13]. Functional disturbances induces in the drug treated cancer

cells could be diagnosed by membrane monitoring as the crucial organelles in cells vital cycle. A diverse range of structurally dissimilar compounds can interact with the tubulin/microtubule system and function as antimitotic agents. These antimitotic agents can be divided into two major classes: those that bind preferentially to α/β-tubulin heterodimers and inhibit polymer assembly, and those with a binding site on the polymer that stabilizes microtubules. Paclitaxel is one of several cytoskeletal drugs that target tubulin. Paclitaxel-treated cells have defects in mitotic spindle assembly, chromosome segregation, and cell division. Paclitaxel has long been recognized to induce mitotic arrest, which leads to cell death in a subset of the arrested population. Chromosomes are thus unable to achieve a metaphase spindle configuration. This blocks the progression of mitosis and prolonged activation of the mitotic checkpoint triggers apoptosis or reversion to the G-phase of the cell cycle without cell division [14]. The ability of paclitaxel to inhibit spindle function is generally attributed to its suppression of microtubule dynamics[15]. Introduced by Brugmans and collaborates in 1971, Mebendazole (Mbz) (methyl5-benzoyl-2-benzimidazole-carbamate) is a prototype benzimidazole carbamate that was initially used for the treatment of intestinal roundworms infections. Mbz exerts its antihelmintic activity primarily by binding to β-tubulin, and inhibiting microtubule polymerization. Mbz binds to helmintic β-tubulin at a higher affinity than mammalian β-tubulin. Thus, it has a selective toxicity and exhibits low adverse effects in humans. Mbz was compared to paclitaxel in a metastatic model of A549 lung cancer cells. Mbz treatment significantly decreased the number of lung colonies compared to paclitaxel and showed lower toxicity[16]. It was noticed that Mbz's binding site is on the outside of the microtubule, which differ from that for paclitaxel and vinblastine, as they bind near the intradiamer interface, facing the lumen of the microtubule[17]. Application of MBZ as an antitubulin depolymerizing

agent [18][19] in treating many types of cancers such as lung cancer [20], gastric cancer [21] and colon cancer [22] were also reported.

Here, a bioelectronics sensor has been developed for noninvasive monitoring the effect of anticancer drugs on single cancer cells based on nano-roughened quartz substrate equipped with gold nanolayer microelectrodes. Whole of the surface except a microcircle surrounded the sensing region of couple microelectrodes was passivated by overbaked photoresist layer (had been applied in microlithography of the sensor). A noticeable population of the cells was dropped to be seeded on the surface of the substrate and locating the cell in a desired place is not a problem in this approach. The seeded MCF-7 cancer cells were exposed to known concentration of anticancer drugs which induced polymerization (PTX(Paclitaxel)) [23][24] and depolymerization (MBZ(Mebendazole))[20] in tubulin structure of the cancer cells. The electrical signals were recorded before and after drug treatment up to 48hrs. Also optical and confocal imaging were investigated to highlight the biological translation of electrical pattern achieved from cancer cells. Several approaches are currently used to manipulate cells on chips. Asphahani et al. reported Single-cell bioelectrical impedance platform for monitoring cellular response to drug treatment through ligand-mediated cell adhesion[25]. J.-L. Hong et al. reported Electrical characteristics analysis of various cancer cells using a microfluidic device based on single-cell impedance measurement[26]. Their work was based on the electrical driving force to fix the location of the cells but it may induce alteration in the cells based on electrical field in the first step. Moreover, M.R. Dusseiller et al. investigated an inverted microcontact printing method on topographically structured polystyrene chips for arrayed micro-3-D culturing of single cells [27]. Their fabrication process was very complicated (about 7 sequential steps) either in constructing the cell adhesion layer or forming electrodes for signal extraction. In addition, many chemical processes were used

in their fabrication flow. Here, we use nano-roughened quartz substrate instead of ligand-mediated cell adhesion not only to increase the cell adhesion, but also to enhance the resolution of signal extraction process for detecting the trace of drug treatment in lower doses. nano-roughened surface was used as electrodes and an overbaked photo resist as passivation layer to capture and extract signal from the cells. Just the tips of the electrodes are exposed to the cell contained solution and other regions were passivized by the polymer layer. These micro cavities surrounded each electrodes also prepare a suitable space for preferential adhesion of the cells in comparison with resist covered regions. Simple fabrication process, easy usage and direct signal extraction are the specification of this method.

2. Material and Methods

2.1 Fabrication of biosensor

The quartz samples as a substrate were cleaned through piranha solutions which are a mixture of concentrated sulfuric acid with hydrogen peroxide, in a ratio of 3:1, to remove trace amounts of organic residues from substrates. The cleaned samples were then placed in a 10% buffer HF solution for 15-20 min to create a nano-roughened surface. Nano roughening process induced nano features with diameter of sub 100nm and height of about 100-200nm (AFM (Atomic-force microscopy) image Fig. 1). Subsequently a thin layer of titanium (1-3nm) was deposited on the samples (to improve Au adhesion) and after that another layer of gold (10-15nm) was coated on the titanium layer by RF-sputtering system (Veeco Co.).

The Ti/Au bilayer has been patterned by standard lithography process to form the biosensor electrodes[28]. The samples then were passivated using photoresist to just form a non-passivated circular region around the electrode tips for cell attachment. The thickness of passivation layer is

about 2µm and the micro well which formed around the electrode enhances the probability of only single cell attachment. The samples then overbaked in 110ºC for 45 min to remove the toxic materials from the resist layer. Interaction of the cells by cured overbaked photoresist passivation layer reveal their biocompatibility as experimented by MTT (Fig. S1) and optical imaging from morphology and growth of the cells (Fig. S2). The schematic of the fabrication process, as well as an optical image of the sensor, were shown in Fig. 1.

Fig. 1. Schematics of fabrication process. A1) cleaning the substrate by piranha procedure. B-1) Nanoroughening the surface by HF solution. B2 and B-3) 3D and line profile AFM image of nano roughened surface.. C) Deposition of Ti/Au layer on nanoroughened surface by Sputtring. D-1) Patterning the titanium/gold layer and forming the architecture of electrodes. Also optical images of electrodes with the distance of about 7 um is observable. E) Spin coating of photoresist as passivation layer on the sensor followed by F-1) patterning the resist and formation of sensing region. Optical images of electrodes with patterned passivation layer befor cell attachment is shown. G) Adhesion of the cells on sensing region and signal extraction from the cell attached electrodes. H) Optical images of individual MCF-7 single cells attached on the nanoroughened electrode after dropping the cells solution(t=0). I) zoomed photograph of electrodes after cell attachment at T=2.

2.2 Cell culture

MCF-7 cell lines which acquired from National Cell Bank of Iran (Pasteur Institute) were used in this experiment. The cell line has been separated from grad I human breast tumors. They were maintained at 37ºC (5% CO_2 , 95% clean air) in RPMI-1640 medium (Sigma) supplemented with 5% fetal bovine serum (sigma) and 1% penicillin/ streptomycin (Gibco). The fresh medium was replaced every other day. In order to detach cell from the substrate and become suspension in solution, cells was trypsynized. As performing cell culturing process in the room temperature about 20-22ºC, it should be done in less than 4-6 minutes to minimize the influence of trypsinization.

2.3 Measurement procedure

The samples were maintained in incubator for 4h to reach cells attachment on biosensors surface. MBZ and PTX antitubulin agents were added into the solution with cells in low (2.1 and 0.1nM) and high (10.5 and 1 nM) concentration respectively. The signals were recorded 2, 5, 8, 20, 32 and 44 hours after drug addition in order (6, 9, 12, 24, 32 and 44 hours after the initial drop). 100 sensors have been fabricated on every chip and in each test about 700-800 cells (count with Neubauer slide) were experimented. Our success rate is about 25-35%. But monitoring only rare number of the cells could provide the sufficient data we need to monitor the drug effects as the electrodes are working independent from each other.

Measurements were collected in frequencies ranged from 1KHz to 60KHz by impedance measurement system every 2 hr. A small "ac" sinusoidal signal was applied to the sensors. For different frequencies of the "ac" signal, the sensitivity of the sensor would vary which is called as the frequency characteristics. The bias voltage of the system was 40mV which wasn't destructive for cellular metabolism as we reported in our previous works [9] and a series resistance was used as current limiter element. All of the 4 electrodes can be used for signal extraction in 2 states (with up-down or right-left neighbor electrodes). The final result is the average of the several signal extraction from the different sensors on a chip to consider cellular heterogeneity and different positioning of the cells relative to the electrodes and other parameters.

2.4 Confocal imaging

Confocal imaging taken from MBZ and PTX treated samples in high and low doses. Non treated samples were imaged as CTRL for comparison. Samples were washed with PBS and permeablized with microtubule stabilizing buffer [80 mM PIPES-KOH (pH 6.8), 5 mM EGTA, and 1mM $MgCl_2$

containing 0.5% Triton X-100] for 5 min at room temperature before being fixed with chilled absolute methanol for 10 min at –20°C. Fixed cells were washed and incubated with monoclonal mouse anti-α-tubulin antibody (Sigma) for 1h at room temperature followed by incubation with FITC-conjugated antimouse IgG antibody (Santa Cruz Biotechnology). The stained cells were observed by confocal microscopy (Leica, TCS SP5, Germany).

2.5 MTT assay

The viability of the cells seeded on roughened quartz surface and overbaked photoresist were experimented by 3-(4,5-dimethylthiazol-2-yl)-2,5-diphenyltetra- zolium bromide (MTT) assay conditions[9]. The surface of the device has been sterilized by autoclave before cell seeding process. The MCF-7 cells were attached on surface and after 24hrs, they were removed from the substrate by trypsin and the culture media was added to the cell solution. Subsequently, the cells were placed in the wells of a sterile 96 well micro plate with the same concentration and the MTT protocol was applied on each well. This assay verifies the viability of the cells based on colorimetric measurement. The reduction of yellow tetrazole to purple formazane is related to the ratio of remained live cells. Metabolic activity of the cells depends on the density deviations of this color in the MCF-7 cell solution. In this regard, 10µl of MTT solution with the concentration of 5 mg/µl was added to each well. The wells were incubated for 4h in 5% CO_2 ambient in 37^{o}C. Next, the float materials were removed from the surface of the wells and 100µl of dimethylsulfoxied was added to each well. After 20 min stirring of each well (in order to solving the formazane), the optical absorption of each cell contained well was calculated in 493 nm by micro plate reader system.

3. Results and discussion

Fig. 2. presented the impedance diagram of a MCF-7 single cell seeded between nanoroughened microelectrodes 4hr after dropping the cells contained solution (the No. of experiment=5). After the attachment of the cell on the region between recording electrodes (after 4hr), observable increment in impedance was recorded with respect to media solution covered state (Fig. 2A Red Vs. Blue curve). T parameter was defined as a time merit started after attachment of the cells (t=4 is equal to T=0). DeltaZ is the difference between impedance at 4^{th} hr after cell seeding (equal to T=0) and the $4+x^{th}$ hr (x=2, 5, 8, etc.), divided by the impedance at T=0. We used average impedance of all frequency for comparison. For better following the impedimetric regime, The impedance changes of the cell were plotted in next times (6^{th}, 9^{th}, 12^{th} and 24^{th} hr) with respect to the impedance of the sensor in 4^{th}hr after dropping the cells solution (Fig. 2B). It is observable that the impedance of the sensor exhibited 17%, 40%, 30% and 50% increase in 2^{nd} (Fig. S3.A), 5^{th} (Fig. S3.B), 8^{th} (Fig. S3.C) and 20^{th} hr after the first signal extraction from the seeded single cell respectively. As the first signaling was recorded 4hr after dropping the cells contained solution, The reference point of recording time was changed from 0^{th} hr to 4^{th} hr. So each interval of time indicated in the figures and diagrams (such as T=2, T=4, *etc.*) means the times passed from the 4^{th} hours after dropping the cells on the surface. The rate of impedance enhancement was ascending from T=2 to T=5. After that, the cell exhibited a reduction in the rate of impedance increment (from T=5 to T=8). When cancer cells enter into spreading stage about 7hr after their attachment on the surface they exhibited reduced impedance response. The reason of such reduction related to the changed ratio of membranes fatty acids and phospholipid structures during cancer transformation. This resulted in weaker mechanical and dielectric function of cancer cell membrane transformation and when cancer cells enter to spreading stage, their ability to block the incoming current become weaker than normal cells which could be characterized as beta dispersion

behavior of the cells [29]. In the first steps of the spreading (T=5), cell covers increasing surface of the sensing electrode and cause an increase of the impedance. But as the cancer cell stretched more, membrane current blocking ability decreased due to thinner structure interfaced with the electrodes and current can be passed through it. However the electrode structure and precision (like silicon nano wire or nano-roughened surface) are very important for detection of these fine signals (see Fig. 6). This result is in a well match with the reports (Fig. 2B; Red Vs. Blue curves). From T=8 to T=20 (Fig. 2B Blue Vs. Green curves), the cell continued its impedance increment. Such increase is in a well corroboration with other reports on enhancement of the cells impedance during growth and mitosis [29]. This would be a good calibration for monitoring the impedance response of single cell for further treatment.

Fig. 2. A) Impedance value of non-treated single MCF-7 cells attached between the couple electrodes (4hr after dropping the cell assumed as T=0). B) Impedance changes of CTRL sample in time evolution. The impedance trend was totally increasing except T=5 to T=8.(C) Impedance changes of similar device after treating the cell by MBZ (2.1nM) and (D) MBZ (10nM). Impedance trends were changed to reductive regime. (E) Individual devices treated by PTX(0.1nM) and (F) PTX (1nM) exhibited increased impedance changes in slower rate than CTRL sample.

Sensing mechanism is straightforward and is predominated by dielectric and beta dispersion changes due to the direct attachment and stretch of cells on sensor. Beta dispersion as one of the intrinsic bioelectrical properties of the cell membrane in response to AC electrical excitation is one of the key parameters involved in our diagnosis approach. This phenomenon is related to the ability of a biological cell membrane in filtering out low frequency currents and allowing high frequency ones to pass through. As the cancerous cells have less ability in blocking the current flow into their membrane, the beta dispersion effects are different from healthy cells.

Electrical responses of the individual devices covered by MCF-7 single cells treated by two different concentrations of MBZ (Fig. 2C:2.1nM and Fig. 2D:10nM) for 20hr (between 4^{th} to 20^{th} hr after dropping the cells on the surface) presented dose dependent decrease in impedance of the cells in time evolution. Such reduction in 2.1nM treated sample was about 5%, 10%, 15% and 30% in T= 2, 6, 8 and 20hr.

Impedance reduction was about 15%, 25%, 35% and 45% in the similar time intervals after treating the cell covered electrodes by 10.5nM of MBZ (Fig. 2D). Inducing apoptosis by treatment of MBZ treatment would be one of the major reasons behind such reduced impedance. As we know that apoptotic cells exhibited serious reduction in their impedance. However, the rate of impedance reduction vs. sweeping frequency was sharper in T=20 meanwhile it was so slower in T=2 or 5. Time progression after treating the cells by the drug might sharply presented the drug effect on the dielectric parameter of the cells as a frequency dependent response. Incubating the cell by PTX drug, as MT(microtubule) polymerizing agent, resulted in different electrical behavior from those of treated by MBZ. Time dependent increase in the impedance of PTX treated single cell (Fig. 2E and 2F) was observed with slower rate and values than that of CTRL(control) sample, the impedance increment in PTX(0.1nM) treated sample was 10%, 30% 35% and 45% in T= 2, 5, 8, 20 hr. Such increment in high dose PTX treated sample was 5%, 15% 20% and 25% in similar time intervals. Enhanced density of the MTs, as dielectric macromolecules in the cytoplasm of the cell because of polymerization might block the current through PTX treated cells and increase the impedance responses of the cells. Moreover the impedance increment because of overpolymerized MTs (after PTX treatment) might compensate the impedance reduction resulted by spreading stage. Finally, a monotonously increasing regime was observed in PTX treated cells with both concentration but in different values. Sharp reduction in time evaluated impedance of MBZ cells

and in contrast moderate increment in time evaluated electrical response of PTX treated single cell (in comparison with CTRL sample) might be correlated with pathological effects of Taxol based drugs on cellular metabolism. Because such drugs wouldn't induce noticeable disruption on cellular function before their entrance into mitotic state [23]. As the result, they wouldn't induce serious impedance disruption on the cell in pre mitotic cycles (from T=2 to T=20).

Impedance phase diagram of the sensors were presented in Fig. 3, to clarify the impedance results. As phase part of the impedance values indicated the capacitive and dielectric parameters of the cell, it would be useful to analyze the effect of anticancer drugs on dielectric parameters of single cancer cell. Attachment of single cell between the electrodes induces minus phases in the response of the sensors due to the capacitive properties of the cell membrane (Fig. 3A). The phase value reached to -45^{o} in 60kHz. Adhesion and proliferation of the cell on the electrodes resulted in phase progression in negative regime. Increased impedance of the cell during the proliferation was in a well corroboration with its enhanced phase (in negative regime) in time evolution (Fig. 3B). About 70% increase in absolute phase value of single cell was observed after 20 hr from its attachment on the surface. Apoptotic induction on single cell after treatment by MBZ could be tracked in phase diagram of Fig. 3C as about 30% decreased was recorded for absolute value of the phase in MCF-7 treated by MBZ (2.1nM) after 5 hr from incubation. The phase decrease continued to 50% and 60% in T=8 and 20 respectively. Higher doses of MBZ induced sharper decrease in the impedance phase of the cell as they seriously disturb the membrane dielectric parameters of the cell by entering it in apoptotic phase (Fig. 3D). The phase results of PTX treated single cells were somehow different. Fig. 3E presented the progressive changes in absolute phase of PTX (0.1nM) treated MCF-7 cell. Non disruptive effect (such as apoptotic induction) of PTX in cell membrane, resulted in increment of phase value but in slower rate than for CTRL sample. Increasing the dose

of PTX inducing observable suppression in progressive changes in the cell phase (Fig. 3F). The phase variation of PTX (0.1 Nm) treated single cell was about -40% meanwhile such value was about -30% in PTX(1Nm) treated sample after 20h from drug incubation.

Fig. 3. A) Impedance phase value of non-treated single MCF-7 cells attached between the couple electrodes (4hr after dropping the cell assumed as T=0). B) Phase changes of CTRL sample in time evolution. The phase trend was totally increasing in negative regime indicated the improved capacitive behavior of the response except T=5 to T=8 (enhanced proliferation of single cell). Phase changes of similar device after treating the cell by (C)MBZ (1nM) and (D) MBZ (10nM) in T=0. Trends of changed phase into the reductive regime indicated disrupted dielectric behavior of the cell (apoptotic induction by drug). Individual devices treated by (E) PTX (0.1nM) and (F) PTX (1nM) exhibited increased changes in absolute with slower rate than CTRL sample (non-apoptotic induction but mitotic arrest might be happened in time evolution).

3.1 Proposed mechanism

Each of the devices was considered to be CTRL, MBZ treated and PTX treated in time evolution. Due to averaging of the 5 different experiments, It could be supposed that the morphology and geometry of the cells haven't effect on a cell electrical response. This would corroborate the similar electrical responses extracted from the individual device at T=0. On the other hand, confocal images were taken from CTRL (Fig. 4A-1) MBZ (10.5nM) treated (Fig. 4A-2) and PTX (1nM) treated (Fig. 4A-3) samples 20hr after drug treatment, revealed different effects of the drug on cytoskeletal structure of the cells. CTRL cells exhibited normal mitosis and division of nucleus and cytoskeleton structure with conformal shape and same ratio between new formed cells.

No entrance to even primary cycles of mitosis, degraded distribution of cytoskeleton and monoastered microtubules are observable indications of MBZ treated cells in comparison with CTRL sample. In addition, images of the PTX treated cell indicated the aggregated MTs as

polymerizing effect of Taxol on cytoskeletal structure which induced mitotic arrest in the cell and deformed the nucleus during the mitosis. Such biological changes better elaborated the considerable different electrical responses between CTRL and drug treated cells (attached on the electrodes) in T=20. Perturbed cytoskeletal structure would disturb the cellular functions by activation of some pathways such as caspase 3 or 9 and finally the cells might be arrested in mitotic cycle or entered to apoptosis before any growth.

Fig. 4. The confocal images of CTRL (A-1 and B-1) MBZ treated (A-2- and B-2) and PTX treated (A-3 and B-3) cells 20hr after drug treatment are observable.

To more elaborate the comparative effect of similar doses of MBZ and PTX on electrical response of treated cells, 1.5nM of both drugs were individually exposed to similar cell covered sensors and the results were determined in T=2, 5, 8, 20, 32 and 44. As it can be seen in part A and B of figure 5, PTX drug induced impedance increment due to MT polymerization up to T=32. After that, the cells completely entered to apoptosis and death induced reduction in the impedance could be observed. As it can be seen in Fig. 5.C and 5.D, MBZ induce decrease in the impedance of treated cells which the impedance reduction was severe in time progression as discussed above. MT depolymerization and perturbing the cell vital cycles (which mediated the apoptosis) induced by MBZ treatment resulted in reduced impedance of treated cells. It can be inferred that with the same dose of drugs, PTX and MBZ induce their own changing regime on cell's electrical response due to their different biological effects.

Fig. 5. Impedance and phase changes of single MCF-7 cells after treating the cell by PTX (A and B) and MBZ (C and D) 1.5nM for T=2, 5, 8, 20, 32, 44.

Fig. 6 presented the mean impedance changes of the single cells treated by various doses of the drugs in comparative style. Time dependent behavior of non-treated cells (red columns) showed

continues increment in impedance (except in spreading stage). Treating the cells with MBZ induced continues reduction in the impedance which exhibited dose dependent linier correlation (MBZ 2.1nM: Blue columns, MBZ 10nM: grey column). By such kind of presentation, just a fast look is enough to realize the reductive effect of MBZ on cells impedance. PTX treated cells showed moderate impedance increment with dose dependent reductive regime (PTX 0.1nM: green column, PTX 1nM: light yellow column). This would corroborate non apoptotic effect of PTX on MCF-7 cells. Similarly, the mean changes in impedance phases of each sample were presented in Fig. 6B. As it was expected, the CTRL samples exhibited progressive phases in negative regime after 24hr. In contrast, apoptotic induction of MBZ turned the phase of the singles cells to positive regimes with dose dependent increasing rate in time evolution. PTX treatment maintained the phase values in negative regime with slower rate than CTRL sample because of capacitive perturbations induced in the cells as the result of mitotic arrest.

To elaborate the effect of nano roughening on the precision of the measurement and sensor sensitivity, the average impedance of the nanoroughened electrode measured at the frequency of 4kHz (presented in Fig. 6A and 6B) was compared by that in smooth electrode (Fig. 6C and 6D). The impedances in all of swap frequencies were calculated and the mean value was extracted by assigning the sharper difference in impedance (in lower frequency) in similar weight to slower differences (in higher frequencies). In addition, at least 5 experiments were made to ensure about impact of nanoroughening. As shown in this Fig , the percent of the impedance changes are about 20% greater in nanoroughened electrode. So, nanoscale geometry of the electrodes plays a crucial role in a detection mechanism and sensor precision.

the greater impedance achieved by nanoroughened electrodes was the result of increased contact sites between cells and electrodes (achieved by nanoroughening the substrate). We reported before

that nanoroughened Silicon surface (named as silicon nanograss structures) [30] increased the contact sites between attached cells and substrate. Similarly, direct contact sites applied between tips of nano roughened features (induced on the quartz surface) and cell membrane, would reduce the gap between cell and electrode surface (Fig. 6-A) and restrict the current flow through media solution. Hence, it would result in improving the role of cell impedance in final response. As the result, the effective interactive surface between cells and substrate was enhanced. So any changes in betas dispersion [30] occurred in the cells transferred to the substrate. Determined impedance changes based on the mentioned biological phenomena were 20% sharper in nanoroughened electrodes.

Fig. 6. Average changes of impedance and phase values for single MCF-7 cells (derived from mean value in all of swap frequencies) treated by different doses of PTX and MBZ by (A, B) nanoroughened and (C, D) smooth sensor in the frequency of 4kHz. Apoptotic induction of MBZ reduced the impedance and increased the phase real values meanwhile mitotic arrest occurred by PTX treatment induce so mild and time consuming disruptive effect on bioelectrical response of the cell.

4. Conclusion

In summary, an electrical biosensor was fabricated by a simple method to electrically monitor the effect of anticancer drugs on breast cancer cell. The electrodes were fabricated on Nano roughened quartz surface and passivated by overbaked photoresist layer. Treating the cell by depolymerizing (MBZ) and Polymerizing (PTX) drugs induced different changes in impedance response of the sensor which exhibited a well correlation with biological effect of such drugs on the cells. Confocal microscopy images indicated the effect of the drug on MT distribution. In the future steps, detecting the cancer metastasis and fabrication of an organ-on a chip for drug resistance assays could be conducted due to the results achieved by this investigation.

References

[1] S.A. Hosseini, M. Abdolahad, S. Zanganeh, M. Dahmardeh, M. Gharooni, H. Abiri, A. Alikhani, S. Mohajerzadeh, O. Mashinchian, Nanoelectromechanical Chip (NELMEC) Combination of Nanoelectronics and Microfluidics to Diagnose Epithelial and Mesenchymal Circulating Tumor Cells from Leukocytes., Small. (2016). doi:10.1002/smll.201502808.

[2] K.R. Schulz, E.A. Danna, P.O. Krutzik, G.P. Nolan, Single-cell phospho-protein analysis by flow cytometry., Curr. Protoc. Immunol. Chapter 8 (2007) Unit 8.17. doi:10.1002/0471142735.im0817s78.

[3] K.D. Gibbs, P.M. Gilbert, K. Sachs, F. Zhao, Single-cell phospho-specific flow cytometric analysis demonstrates biochemical and functional heterogeneity in human hematopoietic stem and progenitor compartments., Blood. 117 (2011) 4226–33. doi:10.1182/blood-2010-07-298232.

[4] R.J. Swain, M.M. Stevens, Raman microspectroscopy for non-invasive biochemical analysis of single cells., Biochem. Soc. Trans. 35 (2007) 544–9. doi:10.1042/BST0350544.

[5] F. Xing, G.-X. Meng, Q. Zhang, L.-T. Pan, P. Wang, Z.-B. Liu, W.-S. Jiang, Y. Chen, J.-G. Tian, Ultrasensitive Flow Sensing of a Single Cell Using Graphene-Based Optical Sensors, Nano Lett. 14 (2014) 3563–3569. doi:10.1021/nl5012036.

[6] E.J. Masicampo, R.F. Baumeister, Conscious thought does not guide moment-to-moment actions-it serves social and cultural functions, Front. Psychol. 4 (2013) 1–5. doi:10.3389/fpsyg.2013.00478.

[7] A. Kouzuma, H. Oba, N. Tajima, K. Hashimoto, Electrochemical selection and characterization of a high current-generating Shewanella oneidensis mutant with altered cell-surface morphology and biofilm-related gene expression, BMC Microbiol. 14 (2014) 190. doi:10.1186/1471-2180-14-190.

[8] Y. Zhao, M. Jiang, D. Chen, X. Zhao, C. Xue, R. Hao, W. Yue, J. Wang, J. Chen, Single-Cell Electrical Phenotyping Enabling the Classification of Mouse Tumor Samples, Sci. Rep. 6 (2016) 19487. doi:10.1038/srep19487.

[9] M. Abdolahad, M. Janmaleki, M. Taghinejad, H. Taghnejad, F. Salehi, S. Mohajerzadeh, Single-cell resolution diagnosis of cancer cells by carbon nanotube electrical spectroscopy, Nanoscale. 5 (2013) 3421. doi:10.1039/c3nr33430a.

[10] Y. Zhao, D. Chen, H. Li, Y. Luo, B. Deng, S.-B. Huang, T.-K. Chiu, M.-H. Wu, R. Long, H. Hu, J. Wang, J. Chen, A microfluidic system enabling continuous characterization of specific membrane capacitance and cytoplasm conductivity of single cells in suspension, 2013. doi:10.1016/j.bios.2012.12.035.

[11] J.-W. Wang, M.-H. Wang, L.-S. Jang, Effects of electrode geometry and cell location on single-cell impedance measurement, Biosens. Bioelectron. 25 (2010) 1271–1276. doi:10.1016/j.bios.2009.10.015.

[12] K. Hu, H. Zhou, Y. Liu, Z. Liu, J. Liu, J. Tang, J. Li, J. Zhang, W. Sheng, Y. Zhao, Y. Wu, C. Chen, Hyaluronic acid functional amphipathic and redox-responsive polymer particles for the co-delivery of doxorubicin and cyclopamine to eradicate breast cancer cells and cancer stem cells., Nanoscale. 7 (2015) 8607–18. doi:10.1039/c5nr01084e.

[13] D.J. Sharp, G.C. Rogers, J.M. Scholey, Microtubule motors in mitosis., Nature. 407 (2000) 41–7. doi:10.1038/35024000.

[14] D.A. Brito, Z. Yang, C.L. Rieder, Microtubules do not promote mitotic slippage when the spindle assembly checkpoint cannot be satisfied, J. Cell Biol. 182 (2008) 623–629. doi:10.1083/jcb.200805072.

[15] M.A. Jordan, L. Wilson, Microtubules as a target for anticancer drugs., Nat. Rev. Cancer. 4 (2004) 253–65. doi:10.1038/nrc1317.

[16] J. Sasaki, R. Ramesh, S. Chada, Y. Gomyo, J.A. Roth, T. Mukhopadhyay, The anthelmintic drug mebendazole induces mitotic arrest and apoptosis by depolymerizing tubulin in non-small cell lung cancer cells., Mol. Cancer Ther. 1 (2002) 1201–9. http://www.ncbi.nlm.nih.gov/pubmed/12479701 (accessed October 19, 2016).

[17] T. Mukhopadhyay, J. Sasaki, R. Ramesh, J.A. Roth, Mebendazole elicits a potent antitumor effect on human cancer cell lines both in vitro and in vivo., Clin. Cancer Res. 8 (2002) 2963–9. http://www.ncbi.nlm.nih.gov/pubmed/12231542 (accessed October 19, 2016).

[18] Z. Tan, L. Chen, S. Zhang, Comprehensive Modeling and Discovery of Mebendazole as a Novel TRAF2- and NCK-interacting Kinase Inhibitor, Sci. Rep. 6 (2016) 33534. doi:10.1038/srep33534.

[19] T. Mukhopadhyay, J. Sasaki, R. Ramesh, J.A. Roth, Mebendazole elicits a potent antitumor effect on human cancer cell lines both in vitro and in vivo., Clin. Cancer Res. 8 (2002) 2963–9. doi:10.1016/s0955-0674(96)80044-5.

[20] J. Sasaki, R. Ramesh, S. Chada, Y. Gomyo, J.A. Roth, T. Mukhopadhyay, The anthelmintic drug mebendazole induces mitotic arrest and apoptosis by depolymerizing tubulin in non-small cell lung cancer cells., Mol. Cancer Ther. 1 (2002) 1201–9. doi:10.3322/canjclin.52.1.23.

[21] L.C. Pinto, B.M. Soares, J. de J.V. Pinheiro, G.J. Riggins, P.P. Assump????o, R.M.R. Burbano, R.C. Montenegro, The anthelmintic drug mebendazole inhibits growth, migration and invasion in gastric cancer cell model, Toxicol. Vitr. 29 (2015) 2038–2044. doi:10.1016/j.tiv.2015.08.007.

[22] P. Nygren, M. Fryknäs, B. Ågerup, R. Larsson, Repositioning of the anthelmintic drug mebendazole for the treatment for colon cancer, J. Cancer Res. Clin. Oncol. 139 (2013) 2133–2140. doi:10.1007/s00432-013-1539-5.

[23] M.L. Flores, C. Castilla, R. Ávila, M. Ruiz-Borrego, C. Sáez, M.A. Japón, Paclitaxel sensitivity of breast cancer cells requires efficient mitotic arrest and disruption of Bcl-xL/Bak interaction., Breast Cancer Res. Treat. 133 (2012) 917–28. doi:10.1007/s10549-011-1864-9.

[24] S. Zanganeh, S. Khosravi, N. Namdar, M.H. Amiri, M. Gharooni, M. Abdolahad, Electrochemical approach for monitoring the effect of anti tubulin drugs on breast cancer cells based on silicon nanograss electrodes, Anal. Chim. Acta. 938 (2016) 72–81. doi:10.1016/j.aca.2016.07.042.

[25] F. Asphahani, K. Wang, M. Thein, O. Veiseh, S. Yung, J. Xu, M. Zhang, Single-cell bioelectrical impedance platform for monitoring cellular response to drug treatment., Phys. Biol. 8 (2011) 1–23. doi:10.1088/1478-3975/8/1/015006.

[26] J.-L. Hong, K.-C. Lan, L.-S. Jang, Electrical characteristics analysis of various cancer cells using a microfluidic device based on single-cell impedance measurement, Sensors Actuators B. Chem. 173 (2012) 927–934. doi:10.1016/j.snb.2012.06.046.

[27] M.R. Dusseiller, D. Schlaepfer, M. Koch, R. Kroschewski, M. Textor, An inverted microcontact printing method on topographically structured polystyrene chips for arrayed micro-3-D culturing of single cells, Biomaterials. 26 (2005) 5917–5925. doi:10.1016/j.biomaterials.2005.02.032.

[28] M. Gharooni, A. Chimeh, B. Valizadeh, S. Mohajerzadeh, M. Shahabadi, Correction of positioning error in Talbot lithography under noncoherent illumination, J. Nanophotonics. 8 (2014) 084089. doi:10.1117/1.JNP.8.084089.

[29] H. Abiri, M. Abdolahad, M. Gharooni, S. Ali, M. Janmaleki, S. Azimi, M. Hosseini, S. Mohajerzadeh, Monitoring the spreading stage of lung cells by silicon nanowire electrical cell impedance sensor for cancer detection purposes, Biosens. Bioelectron. 68 (2015) 577–585. doi:10.1016/j.bios.2015.01.057.

[30] M. Abdolahad, H. Shashaani, M. Janmaleki, S. Mohajerzadeh, Silicon nanograss based impedance biosensor for label free detection of rare metastatic cells among primary cancerous colon cells, suitable for more accurate cancer staging, Biosen. Bioelectron 59 (2014) 151-159 doi: 10.1016/j.bios.2014.02.079

Figures:

fig1.

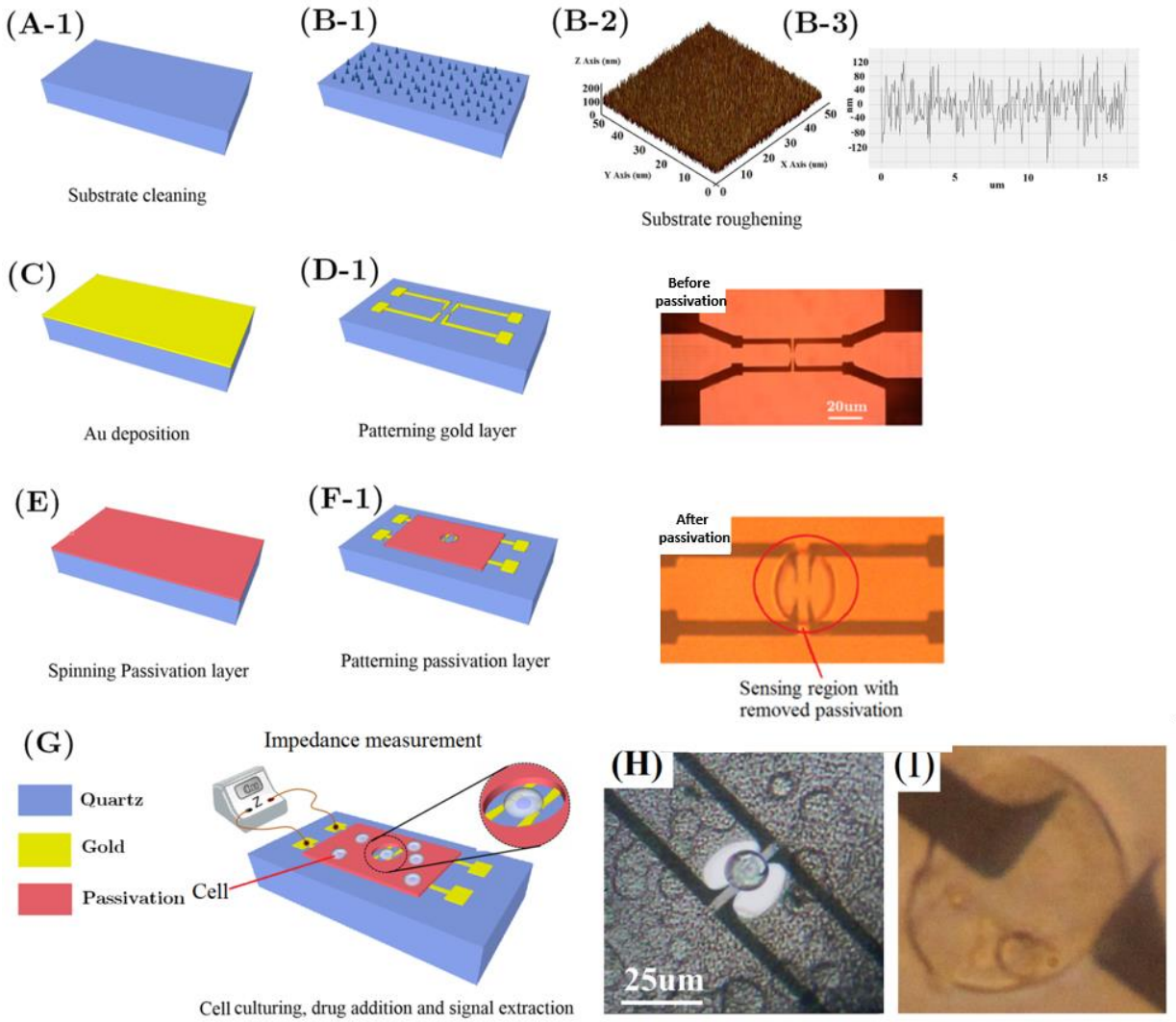

Fig2.

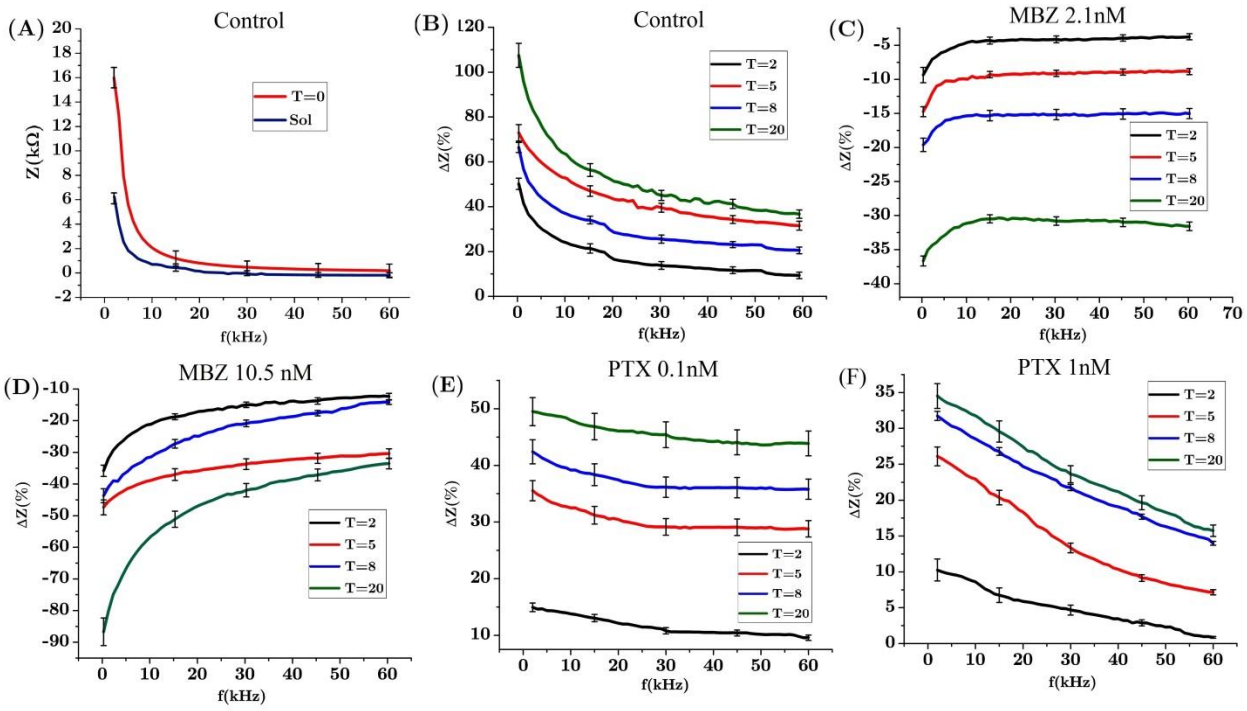

Fig3.

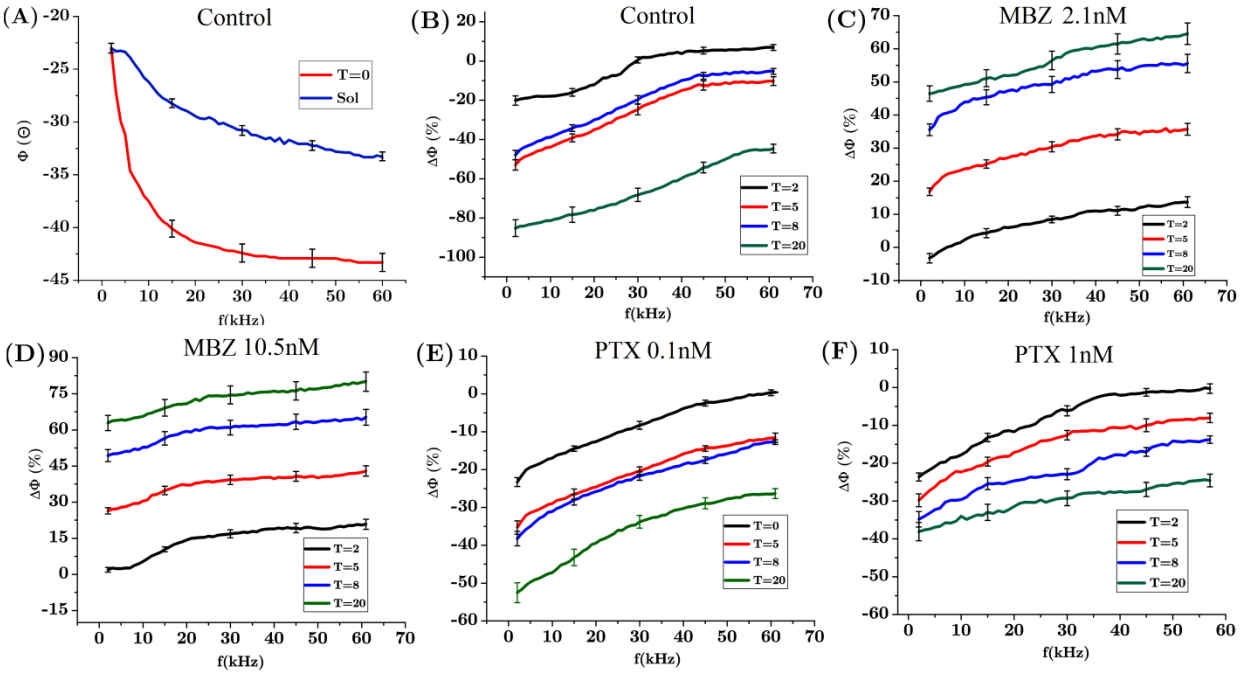

Fig4.

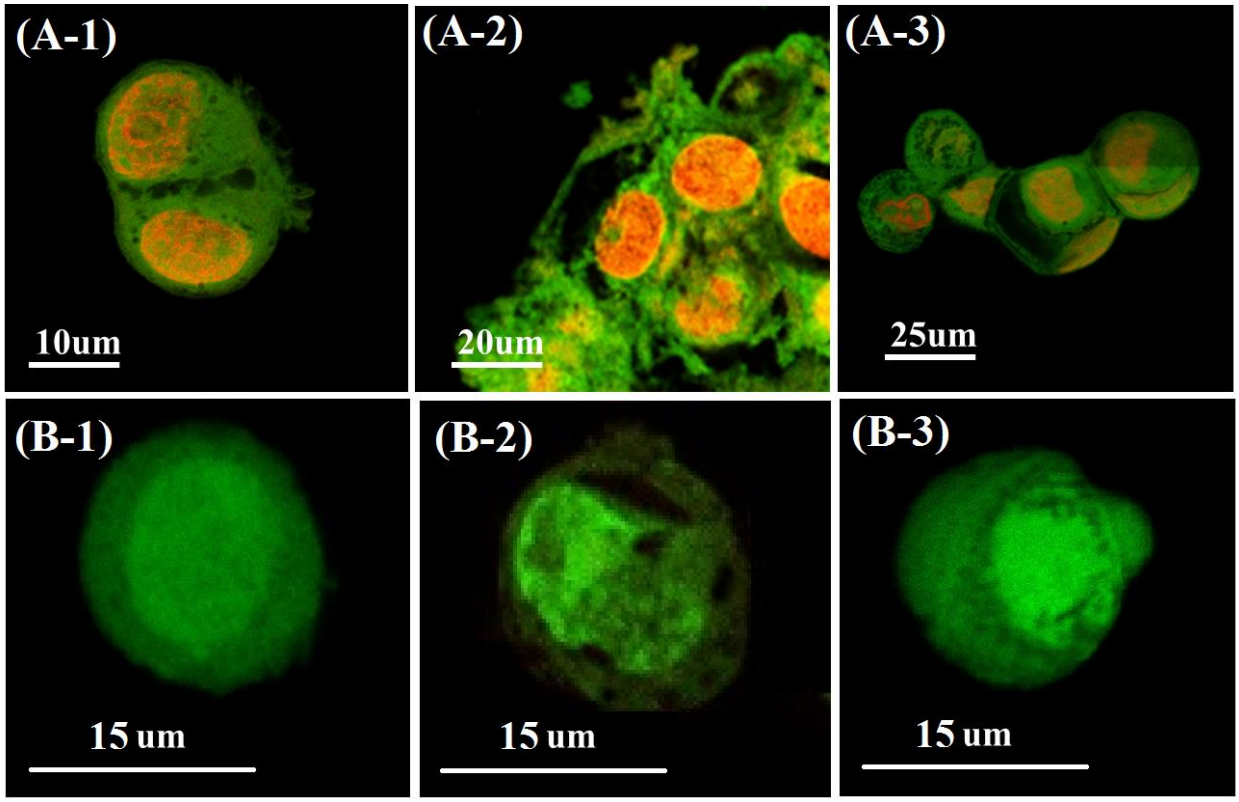

Fig5.

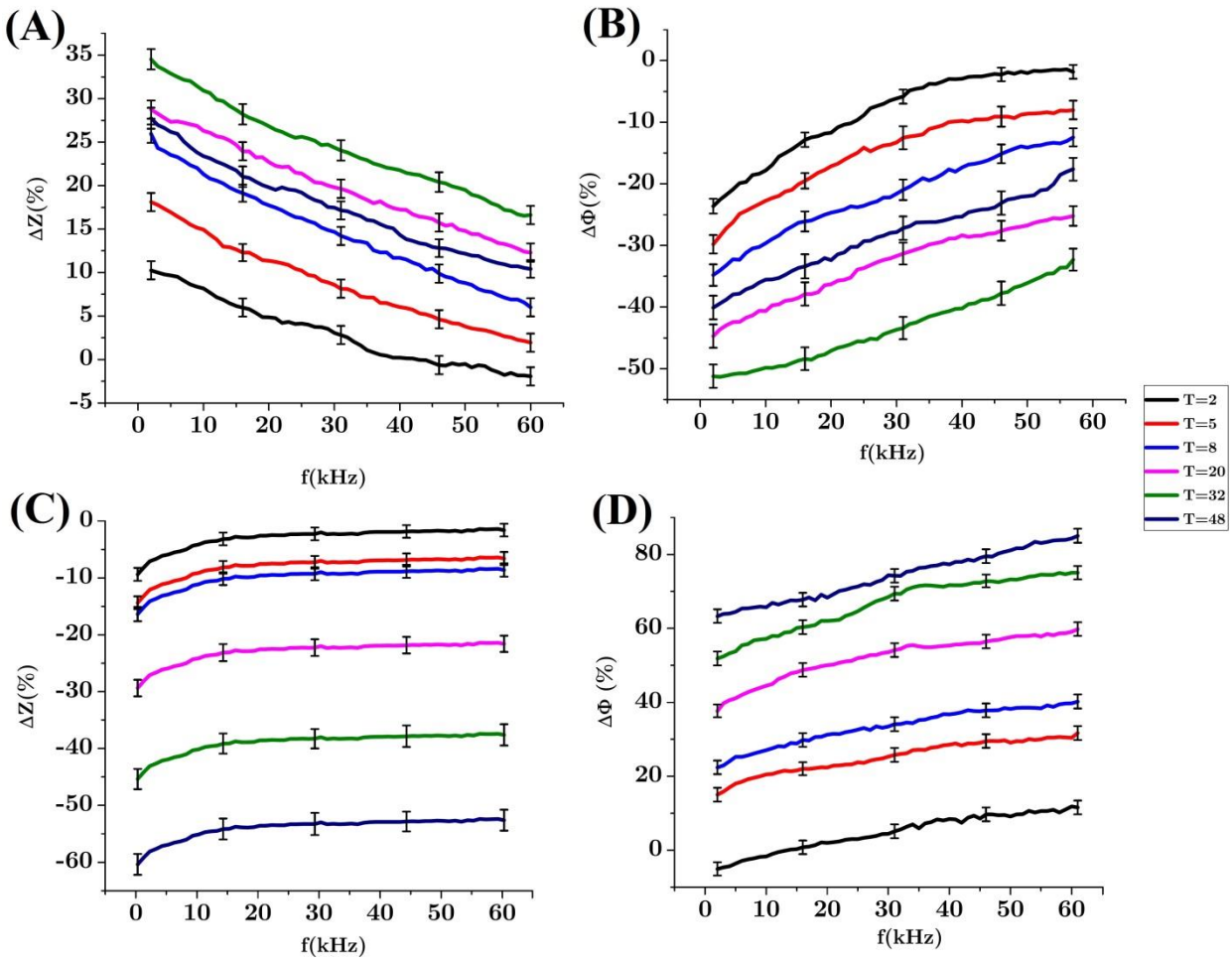

Fig6.